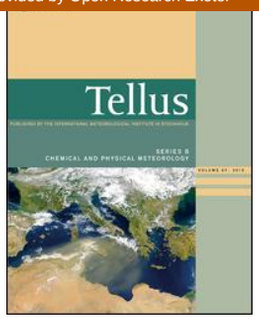

Tellus B: Chemical and Physical Meteorology

ISSN: (Print) 1600-0889 (Online) Journal homepage: http://www.tandfonline.com/loi/zelb20

Nitrate dry deposition in Svalbard

MATSP. Björkman, RAFAEL Kühnel, DANIELG. Partridge, TJARDAJ. Roberts, WENCHE Aas, MAURO Mazzola, ANGELO Viola, ANDY Hodson, JOHAN Ström & ELISABETH Isaksson

To cite this article: MATSP. Björkman, RAFAEL Kühnel, DANIELG. Partridge, TJARDAJ. Roberts, WENCHE Aas, MAURO Mazzola, ANGELO Viola, ANDY Hodson, JOHAN Ström & ELISABETH Isaksson (2013) Nitrate dry deposition in Svalbard, Tellus B: Chemical and Physical Meteorology, 65:1, 19071, DOI: 10.3402/tellusb.v65i0.19071

To link to this article: https://doi.org/10.3402/tellusb.v65i0.19071

Tellus SERIES B CHEMICAL AND PHYSICAL METEOROLOGY
PUBLISHED BY THE INTERNATIONAL METEOROLOGICAL INSTITUTE IN STOCKHOLM

Nitrate dry deposition in Svalbard

By MATS P. BJÖRKMAN[1,2]*, RAFAEL KÜHNEL[1,2], DANIEL G. PARTRIDGE[3,4], TJARDA J. ROBERTS[1,5], WENCHE AAS[6], MAURO MAZZOLA[7], ANGELO VIOLA[8], ANDY HODSON[9], JOHAN STRÖM[3] and ELISABETH ISAKSSON[1], *[1]Norwegian Polar Institute, Fram Centre, N-9296 Tromsø, Norway; [2]Department of Geosciences, University of Oslo, P.O. Box 1047, Blindern, 0316 Oslo, Norway; [3]Department of Applied Environmental Science, Stockholm University, Svante Arrhenius väg 8, SE-11418 Stockholm, Sweden; [4]Atmospheric, Oceanic and Planetary Physics, Department of Physics, University of Oxford, Parks Road, Oxford, OX1 3PU, UK; [5]LPC2E, UMR 7328, CNRS-Université d'Orléans, 3A Avenue de la Recherche Scientifique, 45071 Orléans, Cedex 2, France; [6]NILU – Norwegian Institute for Air Research, Instituttv 18, N-2027 Kjeller, Norway; [7]National Research Council, Institute of Atmospheric Sciences and Climate (ISAC-CNR), Via Gobetti 101, 40129 Bologna, Italy; [8]National Research Council, Institute of Atmospheric Sciences and Climate (ISAC-CNR), Via del Fosso del Cavaliere 100, 00133 Rome, Italy; [9]Department of Geography, University of Sheffield, Sheffield S10 2TN, UK*

(Manuscript received 28 June 2012; in final form 13 November 2012)

ABSTRACT

Arctic regions are generally nutrient limited, receiving an extensive part of their bio-available nitrogen from the deposition of atmospheric reactive nitrogen. Reactive nitrogen oxides, as nitric acid (HNO_3) and nitrate aerosols (p-NO_3), can either be washed out from the atmosphere by precipitation or dry deposited, dissolving to nitrate (NO_3^-). During winter, NO_3^- is accumulated in the snowpack and released as a pulse during spring melt. Quantification of NO_3^- deposition is essential to assess impacts on Arctic terrestrial ecology and for ice core interpretations. However, the individual importance of wet and dry deposition is poorly quantified in the high Arctic regions where in-situ measurements are demanding. In this study, three different methods are employed to quantify NO_3^- dry deposition around the atmospheric and ecosystem monitoring site, Ny-Ålesund, Svalbard, for the winter season (September 2009 to May 2010): (1) A snow tray sampling approach indicates a dry deposition of -10.27 ± 3.84 mg m^{-2} ($\pm$ S.E.); (2) A glacial sampling approach yielded somewhat higher values -30.68 ± 12.00 mg m^{-2}; and (3) Dry deposition was also modelled for HNO_3 and p-NO_3 using atmospheric concentrations and stability observations, resulting in a total combined nitrate dry deposition of -10.76 ± 1.26 mg m^{-2}. The model indicates that deposition primarily occurs via HNO_3 with only a minor contribution by p-NO_3. Modelled median deposition velocities largely explain this difference: 0.63 cm s^{-1} for HNO_3 while p-NO_3 was 0.0025 and 0.16 cm s^{-1} for particle sizes 0.7 and 7 μm, respectively. Overall, the three methods are within two standard errors agreement, attributing an average 14% (total range of 2–44%) of the total nitrate deposition to dry deposition. Dry deposition events were identified in association with elevated atmospheric concentrations, corroborating recent studies that identified episodes of rapid pollution transport and deposition to the Arctic.

Keywords: snow, Arctic, boundary layer, Ny-Ålesund, deposition velocity, nitric acid

1. Introduction

As a result of the industrial revolution and an increasing human population, the concentration of atmospheric reactive nitrogen (N_r) has increased as documented by nitrate concentrations from ice cores around the Northern Hemisphere (Goto-Azuma and Koerner, 2001; Isaksson et al., 2003; Hastings et al., 2009). The N_r enriched air, produced as a result of energy and food production (Galloway et al., 2003), can be subjected to long-range atmospheric transport reaching nutrient-limited Arctic regions, where local pollutions sources are few (Dickerson, 1985). Oxidised nitrogen, mainly originating as nitric oxide (NO) and nitrogen dioxide (NO_2), is transported during

*Corresponding author.
email: mats.p.bjorkman@gmail.com

Citation: Tellus B 2013, **65**, 19071, http://dx.doi.org/10.3402/tellusb.v65i0.19071

winter in the reservoir forms of peroxyacyl nitrates (PANs) and is deposited in the Arctic, after conversion to gaseous nitric acid (HNO_3) or as particulate bound nitrate (p-NO_3) through wet or dry deposition (e.g. Bergin et al., 1995; Seinfeld and Pandis, 2006). The relative importance of these two processes is poorly quantified for Arctic regions, where dry deposition of nitrate compounds is particularly hard to quantify and is the subject of further investigation below.

Arctic regions generally exhibit a deficit of nutrients (Shaver and Chapin, 1980; Nordin et al., 2004; Rinnan et al., 2007). The snow pack, covering up to 50% of the Northern Hemisphere (Barry, 1992; Robinson et al., 1993), works as an efficient winter reservoir for deposited NO_3^-, releasing a concentrated pulse of nutrients during the early stages of snow-melt runoff (e.g. Johannessen et al., 1975; Bales et al., 1989; Goto-Azuma et al., 1994; Lilbaek and Pomeroy, 2008). Atmospheric oxidised nitrogen can reach the ground via wet deposition, in which scavenging by snow or rain leads to HNO_3 and a proportion of p-NO_3 becoming dissolved nitrate (NO_3^-) and follows the precipitation to ground (Barrie, 1991; Diehl et al., 1995; Abbatt, 1997). The large surface area of snowflakes also makes snow highly efficient in scavenging atmospheric pollutants (Barrie, 1991; Abbatt, 1997). Nutrients can also reach the surface via dry deposition, whereby forms of oxidised nitrogen are removed from the atmosphere due to turbulent transfer and gravitational settling with a subsequent uptake of the element at the ground surface (Cadle, 1991), with HNO_3 and p-NO_3 mainly dissolving to form NO_3^- upon contact with the snow cover (Diehl et al., 1995; Abbatt, 1997). The snow cover itself creates an adhesive surface where a thin layer of non-frozen water is present on the surface of each snow crystal, the Quasi Liquid Layer (Kvlividz et al., 1970). Since the snow pack is also a highly permeable material with a constant exchange of air with the atmosphere (Sturm and Johnson, 1991; Albert and Hardy, 1995; Colbeck, 1997; Albert et al., 2002), the process of dry deposition occurs not only at the surface but also within the top few centimetres of the snow pack (Harder et al., 1996).

In the high Arctic region, multiple studies have shown the importance of long-range transport for various pollutants (e.g. Iversen and Joranger, 1985; Barrie, 1986; Stohl, 2006; Hirdman et al., 2010). While there have been a number of model studies describing the transport processes associated with elevated pollutants in the Arctic atmosphere, there have been few studies of the transport processes related to pollutant deposition, and on-site measurements of wet and dry deposition are scarce. Recently, Kühnel et al. (2011) performed a study in Ny-Ålesund, Svalbard, showing that a few precipitation events strongly influence the annual load of NO_3^- and ammonium, NH_4^+, while the majority of precipitation events contributed to a steady base line. Consequently, the ratio between wet and dry deposition is highly dependent on the amount of precipitation in the region (Cadle, 1991), but also dependent on the distance from urban areas where dry deposition likely dominates due to the high concentrations in these more polluted environments (e.g. Forland and Gjessing, 1975). Even though wet deposition seems to be the major nitrogen source (Beine et al., 2003), up to 93% of the total deposition in some Arctic regions (Bergin et al., 1995), dry deposition is still of importance in areas with low precipitation and has been estimated to contribute up to 40% of the total nitrate deposition for sites on Greenland (Fischer and Wagenbach, 1996). Dry deposition is a continuous process and also occurs during precipitation: it has been suggested it contributes up to 10% of the total nitrogen load during a snow event (Beine et al., 2003).

The process of dry deposition depends on the atmospheric concentration of the element and its deposition velocity, v_d, which is influenced by the atmospheric resistance, boundary layer stability and surface structure (Cadle, 1991, cf. section 2.4 and 2.5). Previous studies have measured variable values for v_d onto snow, with v_d for HNO_3 ranging from nearly null values (Johansson and Granat, 1986; Cress et al., 1995) up to several hundred cm s^{-1} (Dibb et al., 1998), with a more commonly used value of 1–2 cm s^{-1} (both measured and modelled data) (Cadle et al., 1985; Cress et al., 1995; Dibb et al., 1998; Wesely and Hicks, 2000; Rattray and Sievering, 2001). Reported measured and modelled values indicate that p-NO_3 has a somewhat more limited range in v_d to snow, from close to zero (Ibrahim et al., 1983; Bergin et al., 1995; Nilsson and Rannik, 2001) to around 4 cm s^{-1} (Cress et al., 1995; Rattray and Sievering, 2001), where the v_d of p-NO_3 is strongly dependent on the size of the particle the nitrate is associated with (Seinfeld and Pandis, 2006). Deposition velocity to snow is also known to be temperature dependent for HNO_3 among other species, where a low v_d is estimated at colder temperatures (Granat and Johansson, 1983; Johansson and Granat, 1986). Earlier investigations of HNO_3 dry deposition in Ny-Ålesund, Svalbard, using denuder filters in a gradient measurement, showed values of 0.012 mg m^{-2} day^{-1} during a 25-d Spring campaign in 2001 where the measured dry deposition was suggested to be associated with the binding of NO_3^- in alkaline snow (Beine et al., 2003). It should also be mentioned that post depositional processes, such as evaporation (Blunier et al., 2005) and photolysis (Honrath et al., 1999), might affect the nitrate budget in the snow, creating gaseous nitric oxide and nitrogen dioxide that can diffuse out of the snow pack and return to the atmosphere (Honrath et al., 2002; Grannas et al., 2007; Jacobi and Hilker, 2007).

The specific aims of this paper are to quantify nitrate dry deposition and its relative importance to the total

atmospheric nitrate deposition in the high Arctic region of Ny-Ålesund, Svalbard. To create a robust estimate, three different approaches were used: first, a simple snow sampling protocol (*Snow Tray*) was used to measure nitrate dry deposition during a spring field campaign; second, snow accumulated during the winter 2009–2010 was excavated from a glacier (*Glacial Accumulation*) to evaluate both total and dry deposition; third, boundary layer stabilities and atmospheric HNO_3 and p-NO_3 concentrations were used to model deposition velocities and dry deposition flux (*Modelling*). The paper also presents detailed method descriptions in order to facilitate future studies in this subject area.

2. Methods

2.1. Site description, climate and data

This study was performed in the high Arctic surroundings of the research facilities in Ny-Ålesund, Svalbard (78°55′N, 11°58′E), where the average (1961–1990) annual temperature is -6.3 ± 1.4 °C with February the coldest month (-14.6 ± 3.4 °C) and July the warmest (4.9 ± 0.8 °C) (Førland et al., 1997). The average annual precipitation in the Svalbard archipelago ranges from 190 to 525 mm. Ny-Ålesund has an annual precipitation of 385 mm and shows greatest precipitation in August–October and March, while May–June receives the least (Førland et al., 1997).

All snow measurements in this study were conducted on the glacier, Austre Brøggerbreen, a few kilometres outside the research village (Fig. 1). Atmospheric concentrations of HNO_3 and p-NO_3 were measured by Norwegian Institute for Air Research[1] (NILU) (Aas et al., 2011). Aerosol size distribution was monitored by the Department of Applied Environmental Science (ITM), Stockholm University. Both atmospheric concentrations and aerosol size distribution were measured at the Zeppelin atmospheric monitoring station at 475 m.a.s.l. (Fig. 1) maintained by the Norwegian Polar Institute (NPI). Meteorological data was provided by the Norwegian Meteorological Institute[2] (DNMI), conducting basic meteorological observations in Ny-Ålesund through NPI, and the Institute for Atmospheric Science and Climate – National Research Council of Italy (ISAC-CNR), conducting atmospheric stability monitoring at the Amundsen-Nobile Climate Change Tower[3] (Fig. 1).

[1]Data available at: *ebas.nilu.no*
[2]Data available at: *www.eklima.no*
[3]*http://www.isac.cnr.it/∼radiclim/CCTower*

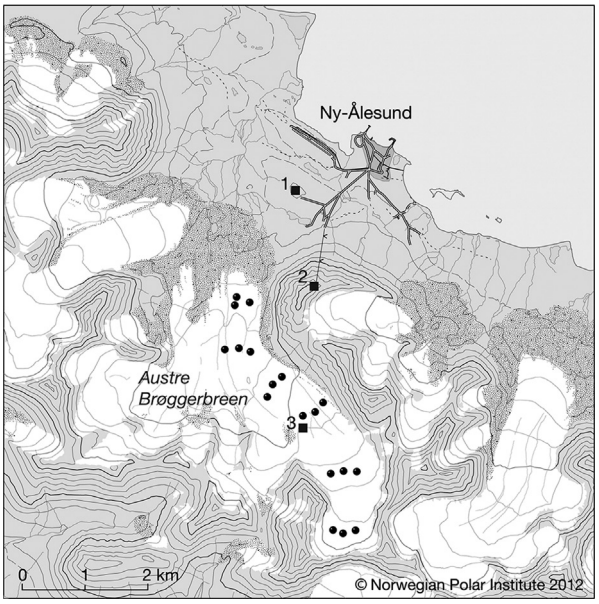

Fig. 1. Map of Ny-Ålesund and Austre Brøggerbreen (Svalbard) with 1) the Amundsen-Nobile Climate Change Tower, 2) Zeppelin atmospheric monitoring station and 3) the *Snow Tray* measurement site. Also included as black circles are the locations where snow samples for the *Glacial Accumulation* method were taken.

2.2. Time periods

For this study, the Winter season was set to cover the period between 10 September 2009 and 4 May 4 2010, starting from when air temperatures dropped below freezing on the glacier and lasting until the final glacial accumulation sampling at Austre Brøggerbreen at the end of the snow pack accumulation season. During Spring 2010 (April 12 to May 5), an intense field campaign using the *Snow Tray* method was conducted and measurements were scaled up to fit the Winter season defined above.

2.3. Measurements

2.3.1. Snow Tray. Dry deposition of dissolved nitrate onto the snow surface was measured during the field campaign on the middle part of Austre Brøggerbreen (Fig. 1) where pre-cleaned PE-plastic trays ($5 \times 25 \times 30$ cm) were used to evaluate nitrate concentration changes in the snow over time (Cadle et al., 1985; Johansson and Granat, 1986; Cadle, 1991; Cress et al., 1995). The plastic trays were filled with surface snow, weighed and then either collected immediately (*zero samples*) or inserted to the snow pack (*exposed samples*) with their exposed snow surface levelled with the surrounding snow. Attention was paid to extract snow for *zero* and *exposed* samples from adjacent locations across a homogenous surface snow using a clean

plastic avalanche shovel, powder-free gloves and clean suite. The *exposed* samples were left inserted in the snow pack for 48–72 h before excavation and weighed a second time. By comparing the concentration and mass of snow in the *zero* and *exposed* samples, post depositional processes in the surface snow, such as dry deposition, can be estimated (Cadle, 1991). Triplicate or quadruplicate samples were performed for the paired zero and exposed samples resulting in a total number of 33 measurements during the Spring campaign. Samples were transferred to clean plastic bags, melted at room temperature overnight, vacuum filtered (0.45 μm filters according to Hodson et al., 2005), bottled and kept frozen for subsequent ion chromatographic analysis. All filter equipment and bottles were triple rinsed with either melted snow samples or ultrapure water and blanks were run along with samples to check for possible contamination.

Anions (NO_3^-, SO_4^{2-}, F^- and Cl^-) and cations (NH_4^+, Na^+, K^+, Ca^{2+} and Mg^{2+}) were measured at the Department of Geography, University of Sheffield, UK, using two separate Dionex DX 90 ion chromatographs, operated through 4400 integrators and AS40 autosamplers. Repeatability for mid-range standards (calibration range: 0 to 2 mg l^{-1}) was 1.6, 5.7, 2.8 and 1.4% for the anions listed above and 2.5, 0.06, 0.2, 0.08 and 1.5% for the cations, respectively. Precision errors deduced from repeat analyses of separate filtered aliquots from a single snow sample were less than 5%. A detection limit of 1 μg l^{-1} was imposed upon all chromatograms using the Chromeleon software, and all analytical blank results were consistently below this limit.

The flux of nitrate to the surface snow, F_{tray}, was obtained from the snow measurements as the change in *total load* per unit area, A, and time, t. The *total load* is defined as the product of the melted snow volume, V, and the concentration of nitrate, c_{NO_3}, in the snow. The flux was corrected for volume changes due new or windblown snow by the term: $c_0(V_0 - V_{exp})$.

$$F_{tray} = \frac{c_0 V_0 - c_{exp} V_{exp} - c_0 (V_0 - V_{exp})}{At} \quad (1)$$

which is equal to:

$$F_{tray} = \frac{c_0 V_{exp} - c_{exp} V_{exp}}{At} \quad (2)$$

where *0* and *exp* denotes the *zero* and *exposed* values, respectively. Hence, with this approach, sampled nitrate will be the total dissolved nitrate in the snow and can come from gaseous HNO_3 or nitrate previously associated with particles.

2.3.2. Glacial Accumulation. Extensive snow sampling was conducted at the end of the 2010 Winter season, from sea level up to 500 m elevation in the Austre Brøggerbreen catchment to evaluate the seasonal dry deposition to the snow. A total number of 27 core samples of the entire snow pack were collected using a core drill (Mark III drill, Kovacs Enterprises Inc.) at the glacier or a cleaned plastic tube at lower elevations. Snow pack density measurements were also conducted at coherent snow pits along the glacial centre line. However, due to frequently occurring melt and storm events, the snow pack at lower elevations (up to 100 m) and closer to the coast was markedly affected and not representative as a seasonal record of snow accumulation. This left 18 samples unaffected and available for analysis (Fig. 1). The snow samples were treated in a similar manner to the snow tray approach, with sample melting and filtration in Ny-Ålesund before freezing and shipment to Sheffield for IC analysis.

The total winter deposition of nitrate to glaciated areas, F_{tot}, can be outlined as a function of wet deposition, F_w, dry deposition, F_d, and other post depositional changes ΔF_p as riming, photolysis or evaporation (Fischer and Wagenbach, 1996; Sharp et al., 2002; Becagli et al., 2005):

$$F_{tot} = F_w + F_d + \Delta F_p \quad (3)$$

Where the wet deposition, $F_w = c_p z_{SWE}$, is dependent on the concentration in the core samples, c_p, and the accumulation, z_{SWE}. In this work, z_{SWE} is referred to as snow water equivalent (SWE) and is given in meters (m). In some areas, photolysis has the potential to influence the nitrate budget (Grannas et al., 2007) while for the Ny-Ålesund region these processes seems to have little influence on the total budget (Beine et al., 2003). If the post depositional changes are set to zero, F_{tot} can be written as (Becagli et al., 2005):

$$F_{tot} = c_p z_{SWE} + F_d \quad (4)$$

By fitting a linear regression between F_{tot} and z_{SWE}, one can calculate the dry deposition, F_d, as the intercept of the regression line with the y-axis (Fischer and Wagenbach, 1996; Sharp et al., 2002; Becagli et al., 2005).

2.4. Modelling

Deposition fluxes can also be calculated using a simplified model including atmospheric concentrations and meteorological data (Hicks et al., 1987; Cadle, 1991; Kumar et al., 2008).

The dry depositional flux, F_{cal}, is described as a function of the deposition velocity, v_d, and the atmospheric concentration, C_{atm} (Seinfeld and Pandis, 2006):

$$F_{cal} = -v_d C_{atm} \quad (5)$$

The atmospheric concentrations of HNO_3 and p-NO_3, C_{HNO_3}, and C_{p-NO_3}, respectively, were measured at a daily resolution by the Norwegian Institute of Air Research (NILU) at the Zeppelin monitoring station using one 3-stage filter pack. Nitric acid is sampled on alkaline impregnated Whatman40 filters and p-NO_3 is sampled on Teflon filters, both analysed by ion chromatography (EMEP, 2001).

2.4.1. Nitric Acid, HNO_3. The deposition velocity for gases can be described as a resistance model combining the aerodynamic-, the quasi laminar boundary layer- and the surface-resistance, r_a, r_b and r_c, respectively**:**

$$v_d(HNO_3) = \frac{1}{r_a + r_b + r_c} \tag{6}$$

The aerodynamic resistance, which has the same value for all substances (Wesely and Hicks, 2000), can be determined for different atmospheric stabilities according to Seinfield and Pandis (2006) by:

$$r_a = \frac{1}{\kappa u*}\left[ln\left(\frac{z_r}{z_0}\right) + 4.7(\zeta_r - \zeta_0)\right] \quad \text{(stable)} \tag{7}$$

$$r_a = \frac{1}{\kappa u*} ln\left(\frac{z_r}{z_0}\right) \quad \text{(neutral)} \tag{8}$$

$$r_a = \frac{1}{\kappa u*}\left[ln\left(\frac{z_r}{z_0}\right) + ln\left(\frac{(\eta_0^2+1)(\eta_0+1)^2}{(\eta_r^2+1)(\eta_r+1)^2}\right) + 2\left(tan^{-1}\eta_r - tan^{-1}\eta_0\right)\right] \quad \text{(unstable)} \tag{9}$$

Where κ is von Karman's constant (equal to 0.4), $u*$ is the friction velocity, z_r is the reference height (10 m in this study) and z_0 the roughness length. Further, $\eta_0 = (1–15\zeta_0)^{1/4}$, $\eta_r = (1–15\zeta_r)^{1/4}$, $\zeta_0 = z_0/L$ and $\zeta_r = z_r/L$ where L is the Monin-Obukhov length.

Hourly-averages of temperature and horizontal velocity, measured at four different heights (2, 4, 10 and 32 m) at the Amundsen-Nobile Climate Change Tower (CCT), were used to evaluate $u*$, z_0 and L.

First, the bulk Richardson number, Ri_m, was estimated at the geometric mean height, z_m, using the logarithmic finite difference approximation for both potential temperature- and wind velocity gradients, $\Delta\theta$ and ΔU, for each consecutive paired heights of observations (2m–4m, 4m–10m, 10m–32m) (Arya, 2001):

$$Ri_m = \frac{g}{T_0}\frac{\Delta\theta z_m}{T_0(\Delta U)^2}\ln\left(\frac{z_{upper}}{z_{lower}}\right) \tag{10}$$

where g is the gravitational acceleration and T_0 the temperature at the lower heights of each observation pair. The potential temperatures were thereby calculated by $\theta = T + (0.0098\ \text{K/m})*z$, were z is the height.

The Monin-Obukhov length was estimated from the Richardson number using the following equations taken from Arya (2001):

$$\frac{z}{L} = Ri,\ for\ \ Ri < 0 \tag{11}$$

$$\frac{z}{L} = \frac{Ri}{1 - 5Ri},\ for\ 0 \le\ \ Ri \le 0.2 \tag{12}$$

For this study, the Richardson number for the lowest paired height ($z_m = 2.83$ m) was used to keep a consistency in the model.

Also the roughness length z_0 and the friction velocity $u*$ can be estimated from the CCT measurements using a profile method (Arya, 2001). The following relation exists between the height of the measurements z, L, $u*$, U and z_0 (Arya, 2001):

$$\ln z - \Psi_m(z/L) = \frac{\kappa}{u*}U + \ln\ z_0 \tag{13}$$

where Ψ_m is the similarity function for the momentum defined by:

$$\Psi_m = -5\frac{z}{L},\ for\ \frac{z}{L} \ge 0 \tag{14}$$

$$\Psi_m = \ln\left[\left(\frac{1+x^2}{2}\right)\left(\frac{1+x}{2}\right)^2\right] - 2\tan^{-1}\eta + \frac{\pi}{2},\ for\frac{z}{L} < 0 \tag{15}$$

with $\eta = (1 - 15\ \zeta)^{1/4}$ and $\zeta = z/L$.

The profile method performs a linear regression between the variables $z - \Psi_m(z/L)$ and U where the slope of the linear regression then corresponds to $\kappa/u*$, while the intercept corresponds to $ln\ z_0$.

Using data from the CCT, it was sometimes difficult to perform a sufficiently good linear regression since wind speeds at the uppermost sensors were occasionally distinctly smaller than the lower levels and lead therefore to poor results. A routine was established to discard wind measurements from top to bottom incrementally until the quality of the regression analysis satisfied the following two criteria: first, the regression needs to have a R^2 value of greater than 0.6; second, the slope of the linear regression needs to be positive, giving a positive friction velocity. The procedure was initiated by performing a linear regression with the wind measurements at all four heights. If the two criteria were not met, the uppermost wind measurement was discarded and the linear regression was repeated. This process was repeated until the criteria were fulfilled or only the bottom wind observation was left, in which case the calculation was aborted leading to missing values.

For successful regressions the friction velocity and roughness length were determined from the regression factors.

The quasi laminar boundary layer resistance can be parameterised as (Seinfeld and Pandis, 2006):

$$r_b = \frac{5Sc^{2/3}}{u*} \tag{16}$$

where Sc is the Schmidt number and can be estimated by $Sc = v/D$ from the kinematic viscosity of air v, estimated with Sutherland's law, and the diffusion constant D. The diffusion constant for HNO_3 was set to 0.118 ± 0.003 cm^2 s^{-1} at a temperature of 298 K and a pressure of 1013.25 hPa (Durham and Stockburger, 1986). For this work the diffusion constant has been corrected for temperature and pressure using the following relation (Massman, 1998):

$$D(T,p) = D(298K,\ 1013.25\,hPa)\left(\frac{p_0}{p}\right)\left(\frac{T}{T_0}\right)^{\alpha} \tag{17}$$

with $\alpha = 1.81$.

The canopy resistance, r_c, for HNO_3 onto snow is commonly assumed to be zero (Cadle, 1991; Wesely and Hicks, 2000; Seinfeld and Pandis, 2006) due to its high affinity to almost any surface (Huebert and Robert, 1985).

2.4.2 Particulate nitrate, p-NO_3. In this study, the particulate dry deposition was calculated following the non-vegetated dry deposition procedure from the EMEP/MSC-E regional model of heavy metals airborne pollution (Gusev et al., 2005; Travnikov and Ilyin, 2005) which uses variations on the resistance analogy approach (Wesely, 1989) for each surface type as documented by Travnikov and Ilyin (2005).

For the particulate deposition, the same simple deposition model [eq. (5)] can be used. However, deriving v_d for particles usually follows a model that also includes the particulate settling velocity, v_s (Seinfeld and Pandis, 2006):

$$v_d(p - NO_3) = \frac{1}{r_a + r_b + r_a r_b v_s} + v_s \tag{18}$$

Note that r_c is not present for particulate deposition, as particles are assumed to stick to any surface upon contact (Seinfeld and Pandis, 2006). Here r_a equals r_a for gases [eqs. (7) to (9)], whereas particulate r_b for non-vegetative surfaces is dependent on κ, $u*$, the wind speed at reference height (10 m), U_{ref}, the Brownian diffusion, E_b, and the impaction, E_{im} (Slinn and Slinn, 1980):

$$r_b = \frac{\kappa U_{ref}}{u_*^2}(E_b + E_{im})^{-1} \tag{19}$$

While E_b can be estimated as $E_b = Sc^{-2/3}$ (Slinn, 1982), the E_{im} is derived from the Stokes number, St, as $E_{im} = 10^{-3/St}$ (Slinn and Slinn, 1980), where St is dependent on $u*$, v_s, g and the kinematic viscosity of air, v, in the following relationship (Travnikov and Ilyin, 2005):

$$St = \frac{u_*^2 v_s}{gv} \tag{20}$$

The settling velocity, v_s, is dependent on the aerosol diameter, d_p, the aerosol density, ρ_p, the Cunningham correction function, G_{cunn}, the air viscosity, η, and g (Travnikov and Ilyin, 2005):

$$v_s = \frac{d_p^2 \rho_p g}{18\eta} G_{cunn} \tag{21}$$

In this study G_{cunn} was based on Allen and Raabe (1982):

$$G_{cunn} = 1 + Kn\left[2.514 + 0.8\exp\left(-\frac{0.55}{Kn}\right)\right] \tag{22}$$

Where the Knudsen number, Kn, is dependent on the mean free path of air molecules, λ, and the d_p of the particles in the following relation $Kn = 2\lambda/d_p$.

The final v_d will be influenced by the d_p of the aerosols of interest, see eqs. (21) and (22), which we estimated in two different ways. Firstly, the particulate size distribution continuously measured by ITM at the Zeppelin Station was used. The custom made Differential Mobility Particle Sizer, DMPS (Ström et al., 2003) delivers aerosols in 40 size bins from 0.01 to 0.89 μm. A volume ratio, $R_{DMPS} = V_{bin}/V_{tot}$, to the total volume of all aerosols was calculated for each size bin, assuming a spherical shape of the aerosols. The DMPS delivers dry aerosol sizes and the v_d used for deposition calculations was therefore calculated for aerosols of a double diameter, $v_{d(2\times Dp)}$ (Zieger et al., 2010). This gave a new d_p size range from 0.02 to 1.78 μm. The dry deposition for the sum of the 40 size bins, F_{p-NO_3}(DMPS), was then calculated using the atmospheric p-NO_3 concentration measured by NILU, C_{p-NO_3}:

$$F_{p-NO_3}(\mathrm{DMPS}) = -\Sigma\left(R_{DMPS} v_{d(2\times Dp)} C_{p-NO_3}\right) \tag{23}$$

However, earlier studies suggest that nitrate in the Ny-Ålesund area is likely associated with sea salt particles with a larger diameter than what is captured by the DMPS (Hara et al., 1999; Teinilä et al., 2003, 2004). For the period investigated in this study there were no continuous measurements of particulate size distributions in the supermicron size in Ny-Ålesund or at the Zeppelin Station. Based on the observations of p-NO_3 among supermicron aerosols in the Arctic by Teinilä et al. (2003) and Bergin et al. (1995), it was assumed that the concentration of nitrate carrying aerosol follows a lognormal distribution (LND); where 99.7% of all the aerosol can be found in the

range between 0.8 and 7 μm (with mean $d_p = 2.37\ \mu m$ and a standard deviation of $\sigma = 0.36$). The total observed aerosol concentrations were distributed into five size bins. The ratio, $R_{LND} = X_{bin}/X_{tot}$, of aerosol in each bin to the total aerosol was calculated from the LND assumption and the corresponding distribution function (Table 1). For each bin the v_d was calculated for the aerosol diameter at the centre point of each bin on a logarithmic scale (Table 1). The dry deposition flux, F_{p-NO_3}(LND), was then calculated as the sum of each individual deposition:

$$F_{p-NO_3}(\mathrm{LND}) = -\Sigma\left(R_{LND} v_d C_{p-NO_3}\right) \quad (24)$$

3. Results and discussion

The results and interpretation of the three methods used are out lined below with a standard error (±S.E.) of the estimates to show the uncertainty of the measurements. Negative numbers are used to denote dry deposition as an atmospheric loss of nitrate, which is equivalent to a surface increase.

3.1. Snow tray measurements

The results from the snow tray measurements show nitrate fluxes, F_{tray}, that ranged from −0.34 to 0.28 mg m^{-2} over the sampling intervals (48–72 h) with two periods indicating a net loss of nitrate from the snow (positive fluxes shown on 20 and 25 April) and seven indicating either a net gain or no net change occurred (Fig. 2a). The F_{tray} during the field campaign indicated an average -0.04 ± 0.03 mg m^{-2} (*full* data) nitrate deposition (p-value of 0.21). When excluding the two periods with clear nitrate loss, the average dry deposition, -0.09 ± 0.03 mg m^{-2} (deposition *only* data), showed significant (p = 0.01) values. Using these data a daily dry deposition flux of -0.02 ± 0.02 mg m^{-2} day^{-1} or -0.04 ± 0.02 mg m^{-2} day^{-1} was established (*full* data or deposition *only* data, respectively). Data collected in this way typically represent the sum of several ongoing processes, including dry deposition (Cadle, 1991), riming (Fischer and Wagenbach, 1996), re-evaporation (Blunier et al., 2005) or photolysis (Grannas et al., 2007). Even though the *full* data are in agreement with an earlier estimate (−0.012 mg m^{-2} day^{-2}) from a study that employed denuder filters and gradient technique (Beine et al., 2003), the dry deposition *only* data are in agreement with a separate study conducted in April 2010 (-0.04 ± 0.01 mg m^{-2} day^{-1}, Björkman et al., unpublished data) that focused on nitrate isotopic signatures in surface snow. The dry deposition *only* data have been chosen to best represent the full accumulation season (10 September 2009 to 4 May 2010) owing to the lack of radiation and cold temperatures during the winter limiting photochemical and re-evaporative loss of nitrate.

Table 1. Model inputs for the log normal distributed (LND) run based on figures provided in Teinilä et al. (2003) and Bergin et al. (1995). Given are the range of each size bin, the particle diameter (d_p) at the middle of each size bin on the logarithmic scale and the individual ratio (R_{LND}) between the size bins following a log normal distribution

Size bin intervals (μm)	d_p (μm)	R_{LND} (%)
0.80–1.23	0.99	3.5
1.23–1.90	1.53	23.8
1.90–2.94	2.37	45.1
2.94–4.54	3.65	23.8
4.54–7.00	5.64	3.5

With this assumption, F_{tray} for the whole period was scaled up to -10.27 ± 3.84 mg m^{-2}, while the spring campaign (April 12 to May 5, 2010) accounted for -1.00 ± 0.37 mg m^{-2} (Table 2). Furthermore, of the 33 original samples, 21 were used in these final calculations; the missing data were due to clear indications of contaminated ultrapure water being used for rinsing, or by samples destroyed during transport.

The measured nitrate concentrations, c_{NO_3}, in the snow fluctuate between 0.05 and 0.18 mg l^{-1}, with the highest concentrations measured on 28 April after three windy days, (Fig. 2b and c). Concentrations in *zero* and *exposed* samples obtained on the same date follow each other closely except for 14, 25 and 28 April 2010 (Fig. 2c). The *total load* of nitrate in the tray, mg m^{-2}, could be calculated using the melted snow volume and nitrate concentration in the snow. The *total load* in Fig. 2b shows an increase during the first six days in both zero and in exposed samples (except 20 April) where the exposed value has been corrected for any change due to wind or snow fall according to the last part of eq. (1). In total, six pairs show an increase and three indicate a decrease. The influence of wind and precipitation events can clearly be seen in the samples obtained on 28 April, where in particular the *total load* of the *zero* snow is highest (Fig. 2b). A weak correlation (R = 0.46) between snow weight changes and F_{tray} indicates that the influence of redistributed snow, due to wind, or newly fallen snow was low. However, precipitation events are known to deliver snow with highly variable nitrate concentrations (Kühnel et al., 2011) and thus might have influenced the snow concentrations on 28 April. The frequent mixing of the upper part of the snow pack by wind made separate snow events hard to distinguish, even if they were readily measured in Ny-Ålesund (see wind speed and precipitation in Fig. 2a and b).

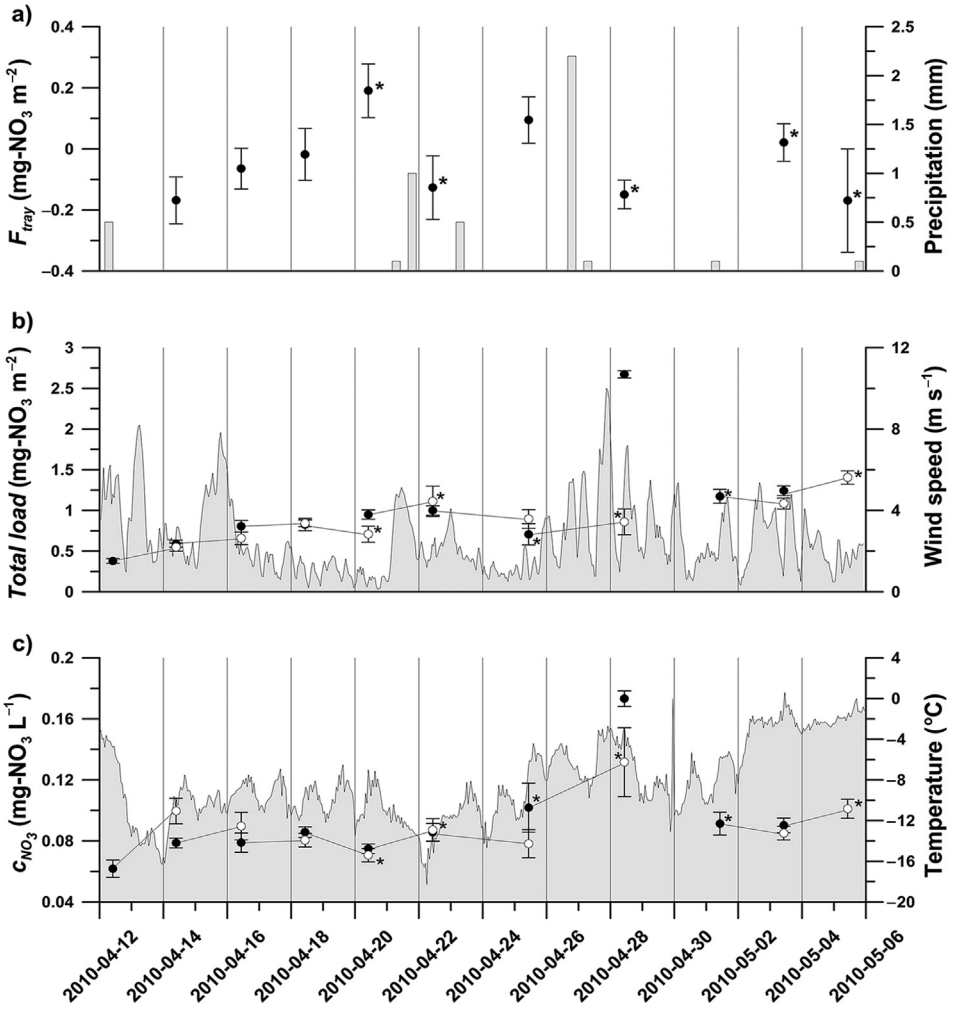

Fig. 2. Dry deposition estimated from *Snow Tray* sampling at Austre Brøggerbreen: a) The calculated NO_3^- flux (F_{tray}) given at the end of each sampling period, where a negative number indicates dry deposition (hence, an atmospheric loss of NO_3^-), b) The calculated *total load* of NO_3^- in the trays, and c) the corresponding NO_3^- concentration (c_{NO_3}) in the snow. Black and white dots indicate the paired *zero* and *exposed* samples, respectively, connected with a straight line for clear identification. Error bars indicate standard error of the measurements, and * indicates standard error calculated from only two data points. Precipitation events, wind speed and temperature measured by DNMI are given as gray bars or shaded areas in a), b) and c).

Table 2. Measured and modelled dry deposition fluxes, mg m^{-2}, for the three different methods used

	Snow tray	Glacial accumulation	Model			Model sum	
	F_{tray}	F_{tot}	F_{HNO_3}	F_{p-NO_3}(DMPS)	F_{p-NO_3}(LND)	DMPS	LND
Accumulation season (10 Sep 2009 to 4 May 2010)							
Dry deposition	-10.27 ± 3.84*	-30.68 ± 12.00	-8.17 ± 1.02	-0.10 ± 0.01	-0.65 ± 0.01	-8.27 ± 1.03	-8.82 ± 1.03
			$-9.97\pm1.25^{\#}$	$-0.12\pm0.01^{¤}$	$-0.79\pm0.01^{\#}$	-10.09 ± 1.26	-10.76 ± 1.26
Spring campaign (12 April to 5 May 2010)							
Dry deposition	-1.00 ± 0.37	–	-0.40 ± 0.08	-0.01 ± 0.001	-0.07 ± 0.001	-0.41 ± 0.08	-0.47 ± 0.08

*To establish a full seasonal estimation the data from the spring campaign have been used and scaled up to fit the glacial accumulation data.
#Data corrected for the 22% paucity.
¤Data corrected for the 25% paucity.

3.2. Glacial accumulation measurements

The load of nitrate, F_{tot}, to the Austre Brøggerbreen snow pack shows a good correlation ($R^2 = 0.78$) to the accumulation where the intercept of a fitted line, F_d, according to eq. (4) indicates a significant nitrate addition of 30.68 ± 12.00 mg m^{-2} ($p = 0.02$) by dry deposition for the winter season (Fig. 3). Hence, this approach emphasizes the net nitrate contribution to the snow pack rather than the loss from the atmosphere. The corresponding atmospheric loss due to dry deposition then equals -30.68 ± 12.00 mg m^{-2}. Along with the snow tray measurements, this approach captures all post depositional processes, see eq. (3), but as mentioned in section 3.1 the long and dark winter at 79° N limits most of the re-emission processes, such that dry deposition is the main influence on the intercept. Furthermore, this method assumes that the snow pack is more or less undisturbed and that the full accumulation season is captured, as has been assumed in earlier studies of high elevation and/or colder sites such as the Greenland ice sheet (Fischer et al., 1998) and Antarctica (Becagli et al., 2005). In particular, rain and melt events are problematic in Ny-Ålesund since the first part of snow melt is known to remove a large proportion of the soluble ions in the snow pack (Brimblecombe et al., 1986; Bales et al., 1989; Kuhn, 2001). During Winter 2009–2010 the lower elevations of the glacial catchment were frequently affected by rain, wind redistribution and melt events, making the snow record invalid as an undisturbed seasonal record for nitrate accumulation; hence, only 18 of the 27 samples were used. Due to this paucity of data in the lower accumulation areas, the uncertainty of the estimated regression line outside the measured values increases, here viewed as the 95% confidence interval shown in Fig. 3; this is important to keep in mind since the reported standard error for the intercept might underestimate the true uncertainty (Fig. 3 and Table 2). It should also be mentioned that the local topography patterns result in a larger accumulation/elevation response than might be expected by the small glacier of Austre Brøggerbreen (Rasmussen and Kohler, 2007). Furthermore, the accumulation for the lowest three samples in Fig. 3 is smaller than in the mass-balance data (Table 4), which also includes superimposed ice, and where the accumulation deviate due to the topography of the underlying glacial ice.

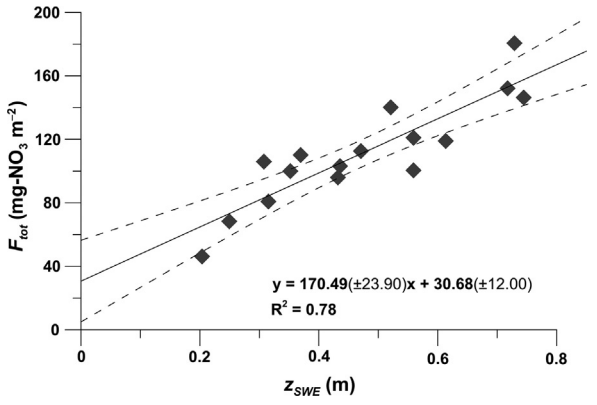

Fig. 3. The load of NO_3^- in the snow pack (F_{tot}), calculated from snow cores capturing the entire winter accumulation at Austre Brøggerbreen, plotted versus the snow accumulation (z_{SWE}). Also given is the linear regression (solid line) for the data where the intercept with the y-axis indicates NO_3^- addition due to dry deposition (F_d). Further, the corresponding 95% confidence interval for the linear model (broken line) is given as well as the equation for the regression line (± 1 S.E.).

Earlier work has shown that orographic clouds can enhance the ionic concentrations in precipitation even in the Arctic (Semb et al., 1984), a phenomena often referred to as the 'seeder feeder effect' (Fowler et al., 1988; Dore et al., 1992a, b). No evidence of such an effect was present in the Austre Brøggerbreen data set, although the process might still affect other parts of the Arctic region.

3.3. Model output

The atmospheric concentrations C_{HNO_3} and C_{p-NO_3} measured at the Zeppelin Station (Fig. 4a and b, respectively) show background values of 0.04 mg-NO_3^- m^{-3} for both gaseous and particles with occasionally higher concentrations, e.g. in the first half of January 2010.

The method adopted for HNO_3 dry deposition, F_{HNO_3}, evaluation generates hourly deposition velocities, v_d, when the required conditions are satisfied (cf. section 2.4.2). A median v_d of 0.63 cm s^{-1} (1st and 3rd quartile on 0.34 and 0.99 cm s^{-1}, respectively) was found for the investigated winter period and the full hourly data set ranged from 0.04 to 3.55 cm s^{-1} (Fig. 5a and Table 3). The median v_d is somewhat lower than earlier observations to snow (Cadle et al., 1985; Dibb et al., 1998) or calculated for vegetations (Wesely and Hicks, 2000; Rattray and Sievering, 2001; Zhang et al., 2009). The v_d was also influenced by the atmospheric stability, Richardson numbers *Ri* (Fig. 6 and Table 3), where the median v_d was 0.80 or 0.22 cm s^{-1} when considering unstable ($R_i < 0$) or stable ($R_i > 0$) conditions separately.

From the atmospheric concentrations, C_{HNO_3}, and the v_d, a daily flux, F_{HNO_3}, was estimated and ranged from values close to zero to up to -1.03 mg m^{-2} day^{-1}, with an overall median of -0.02 mg m^{-2} day^{-1} and 1st and 3rd quartiles of -0.01 and -0.03 mg m^{-2} day^{-1}, respectively (Fig. 5b). The modelled daily F_{HNO_3} showed a strong correlation with C_{HNO_3} ($R = 0.88$) while the correlation with Ri_m was poor ($R = 0.22$). The influence of C_{HNO_3} can also be seen in the deposition event during the first half

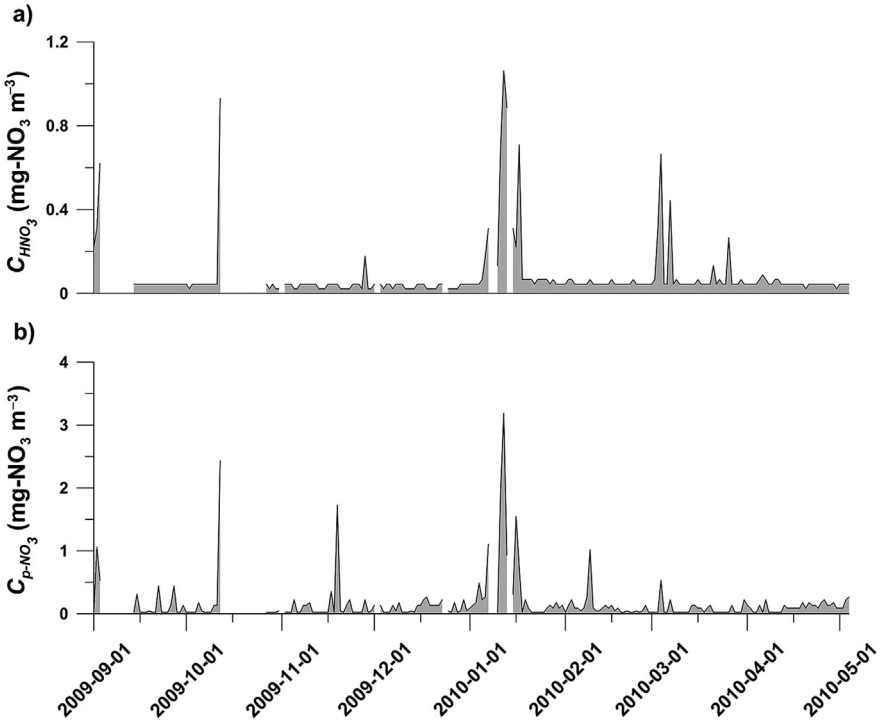

Fig. 4. Measured concentrations of a) gaseous nitrate acid ($C_{\mathrm{HNO_3}}$) and b) particulate nitrate ($C_{\mathrm{p-NO_3}}$) measured by NILU at the Zeppelin atmospheric monitoring station. Gaps in the a) and b) indicates missing data.

January 2010 (Fig. 5b) which corresponds to increased atmospheric concentration during that time (Fig. 4a).

The modelled daily $F_{\mathrm{HNO_3}}$ was strongly influenced by the atmospheric concentration with the highest deposition flux occurring during the first half January 2010 (Fig. 5b). The accumulated $F_{\mathrm{HNO_3}}$ from the atmosphere, here calculated from the daily average flux and standard errors, indicates a total dry deposition of -8.17 ± 1.02 mg m^{-2} during the winter season and -0.40 ± 0.08 mg m^{-2} for the investigated spring field campaign (Fig. 5c and Table 2).

Hourly v_{d} for p-NO_3 varies with the particulate diameter, d_{p}, and the hourly v_{d} produced by the model is summarised in Fig. 7. Generally, the variation in v_{d} is larger among submicron aerosols and shows more consistent values among supermicron particles. The v_{d} for submicron aerosols also tends to be smaller than earlier estimates; i.e. Ibrahim et al. (1983) found v_{d} for particles with a diameter of 0.7 μm to be between 0.039 and 0.096 cm s^{-1} while the median for the same diameter estimated here is one order of magnitude smaller 0.0025 cm s^{-1} (Table 3). Also Petroff and Zhang (2010) indicate higher v_{d} for submicron aerosols in their models. For the supermicron sizes the v_{d} tends to be more in line with Ibrahim et al. (1983) who estimated 0.096 and 0.16 cm s^{-1} for 7 μm particles where the modelled median here is 0.163 cm s^{-1} for the same size (Table 3). The v_{d} for the larger aerosol sizes are also in agreement with numbers previous used for p-NO_3 deposition to smooth surfaces like snow (Cadle et al., 1985; Bergin et al., 1995; Zhang et al., 2009; Petroff and Zhang, 2010). The median v_{d} during stable and unstable atmospheric conditions (upper and lower dashed lines in Fig. 7) indicates that submicron aerosols are more sensitive to the stability regime then supermicron particles. The median daily v_{d} for all size bins in the DMPS and the LND runs of the model (Fig. 8a) shows consistently higher values for the LND run reflecting the higher v_{d} among larger particles. It should be mentioned that previous models for estimating aerosol v_{d} onto snow yield variable results due to the large uncertainties in the many parameters upon which the models are built, for further discussion and comparison of models and measurements please see Petroff and Zhang (2010).

Even though v_{d} varies with time, the dry deposition flux, $F_{\mathrm{p-NO_3}}$, for both the DMPS and the LND runs are poorly correlated with Ri_{m} ($R < 0.20$ for both runs) but shows a strong influence of $C_{\mathrm{p-NO_3}}$ ($R > 0.98$) as can be seen in Figures 4b and 8b. The median daily $F_{\mathrm{p-NO_3}}$ (DMPS) over the winter season was calculated to be -0.186×10^{-3} mg m^{-2} day^{-1} (1st and 3rd quartile on -0.077×10^{-3} and -0.459×10^{-3} mg m^{-2} day^{-1}, respectively), while $F_{\mathrm{p-NO_3}}$(LND) was one order of magnitude higher, -1.211×10^{-3} mg m^{-2} day^{-1} (1st and 3rd quartile on -0.492×10^{-3} and -2.958×10^{-3} mg m^{-2} day^{-1}, respectively). The difference in the daily median deposition

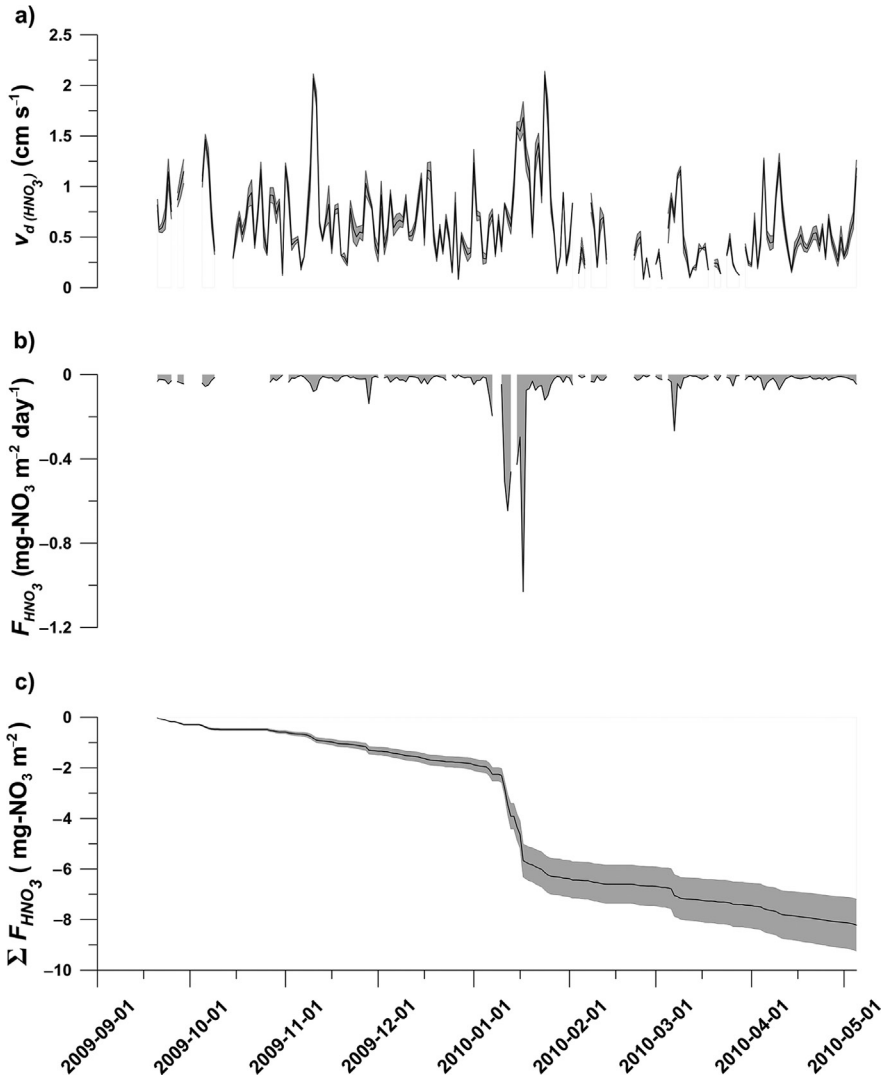

Fig. 5. Modelled dry deposition of HNO_3 during Winter 2009–2010: a) daily average deposition velocity ($v_{d\ (HNO_3)}$) given by the model, b) daily average dry deposition of HNO_3 (F_{HNO_3}) calculated from the C_{HNO_3} (Fig. 4a) and $v_{d\ (HNO_3)}$, and c) the accumulated dry deposition ($\Sigma\ F_{HNO_3}$) giving the total deposition for the winter season. The shaded areas in a) and c) indicate standard error of the estimates, while the shaded area in b) resembles the integrated area for the estimated dry deposition.

leads to a large difference in the accumulated winter deposition where F_{p-NO_3}(DMPS) sums up to -0.095 ± 0.012 mg m^{-2}, whereas F_{p-NO_3}(LND) sums up to -0.649 ± 0.012 mg m^{-2} (Fig. 8c and Table 2). The corresponding estimates for the spring field campaign period were -0.011 ± 0.002 and -0.069 ± 0.001 mg m^{-2} for F_{p-NO_3}(DMPS) and F_{p-NO_3}(LND), respectively (Table 2).

Due to the occasional distinctly smaller wind velocities measured at the upper levels of the CCT, indicating a very shallow boundary layer, and also the occasional absence of atmospheric concentration estimates, the loss of modelled hourly data was up to 63% for the F_{HNO_3} method during the winter season. For F_{p-NO_3}, 66 and 63% of the hourly data were missing (DMPS and LND, respectively) due to the same reason. Since daily averages have been used for the calculations the lack of hourly data was smoothed out, resulting in 22% of HNO_3 data and 25 or 22% paucity of p-NO_3 data (DMPS and LND, respectively) missing in the final winter season sum up. This indicates that the actual dry deposition for HNO_3 and p-NO_3 could be up to -9.972 ± 1.245 mg m^{-2} for HNO_3, while p-NO_3 for the DMPS and LND runs was -0.118 ± 0.011 and -0.791 ± 0.014 mg m^{-2} (Table 2). For the spring campaign, there was a 50% paucity of hourly data, while daily average data coverage was complete, thus no correction was needed.

The total modelled dry deposition ($F_{HNO_3} + F_{p-NO_3}$) during winter 2009 to 2010 was between -10.09 ± 1.26 and -10.76 ± 1.26 mg m^{-2} using the DMPS and the LND

Table 3. Summary of model output for the roughness length z_0, friction velocity u_*, Richardson number Ri_m, aerodynamic resistance r_a, quasi laminar boundary layer resistance r_b for gaseous nitric acid HNO_3, and particulate nitrate p-NO_3, together with deposition velocities v_d

						$r_{b\ (p-NO_3)}$			$v_{d\ (p-NO_3)}$	
	z_0 (m)	u_* (m s^{-1})	Ri_m	r_a (s m^{-1})	$r_{b\ (HNO_3)}$ (s m^{-1})	(DMPS) (s m^{-1})	(LND) (s m^{-1})	$v_{d\ (HNO_3)}$ (cm s^{-1})	0.7 μm (cm s^{-1})	7 μm (cm s^{-1})
Min	0.00	0.10*	−2.95	10.19	13.63	1.75	939.08	0.04	0.0020	0.155
1st Quartile	5.09×10^{-6}	0.10	−0.15	63.91	34.82	5597.70	1.62×10^{7}	0.34	0.0023	0.160
Median	4.28×10^{-4}	0.21	−0.02	107.45	54.57	2.28×10^{4}	3.72×10^{7}	0.63	0.0025	0.163
3rd Quartile	0.01	0.32	0.12	207.81	105.03	8.18×10^{4}	7.96×10^{7}	0.99	0.0029	0.189
Max	5.93	0.78	1.98	1000#	124.51	1.85×10^{6}	6.93×10^{8}	3.55	0.0413	4.097

*For this work u_* was given upper and lower boundaries of 0.10 and 1.5 m s^{-1}, respectively.
#For this work R_a was given upper and lower boundaries of 10 and 1000 s m^{-1}, respectively.

data sets, respectively (Table 2). For the spring field campaign the estimated dry deposition was found to be -0.41 ± 0.08 and -0.47 ± 0.08 mg m^{-2}, for DMPS and LND, respectively (Table 2). Even though the two model p-NO_3 data sets differ substantially, they only accounted for between 1 and 7% of the total modelled dry deposition in this study, attributing the majority of dry deposition to HNO_3, as recorded by previous studies (Cadle et al., 1985; Zhang et al., 2009; Osada et al., 2010). Hence, even adapting the model to fit the submicron $v_{d\ (p-NO_3)}$ previous reported in literature (Petroff and Zhang, 2010 and references there in) would not change this relationship. Taking earlier literature v_d estimations (Cadle et al., 1985; Bergin et al., 1995; Nilsson and Rannik, 2001; Zhang et al., 2009) and d_p of p-NO_3 in the Arctic (Bergin et al., 1995; Hara et al., 1999; Ianniello et al., 2002; Teinilä et al., 2003; Teinilä et al., 2004) into account, the modelled results from the LND run seem to best represent the actual p-NO_3 deposition in the Ny-Ålesund area and will be the one used for further discussion in this work.

It has also been common in earlier studies to use a fixed number for the roughness length (z_0) when establishing a model, usually 0.01 m for snow (e.g. Seinfeld and Pandis, 2006). The method applied in this work uses the CCT data to also evaluate z_0, with values in the range from zero to those of a high elevated skylines in central business districts (Seinfeld and Pandis, 2006) (i.e. at two occasions the hourly values exceed 4 m, Table 3). The median z_0 of 4.28×10^{-4} m is in line with observations by Ibrahim et al. (1983) for snow. In addition, the friction velocities (u_*) estimated with this model, median 0.21 m s^{-1} (Table 3), are within the range of earlier studies on snow (Ibrahim et al., 1983). Markedly, the aerodynamic resistance (r_a) is of the same order as the estimated boundary resistance (r_b) for gaseous HNO_3 (1st quartile at 63.91 and 34.82 s m^{-1}, 3rd quartile at 207.81 and 105.03 s m^{-1}, respectively), giving the both resistances a similar impact on the dry deposition flux. The median particulate r_b is in the order of three magnitudes higher, 2.28×10^{4} s m^{-1} for the DMPS run and 3.72×10^{7} s m^{-1} for the LND run, and by far seems to be the restricting factor for p-NO_3 dry deposition (Table 3).

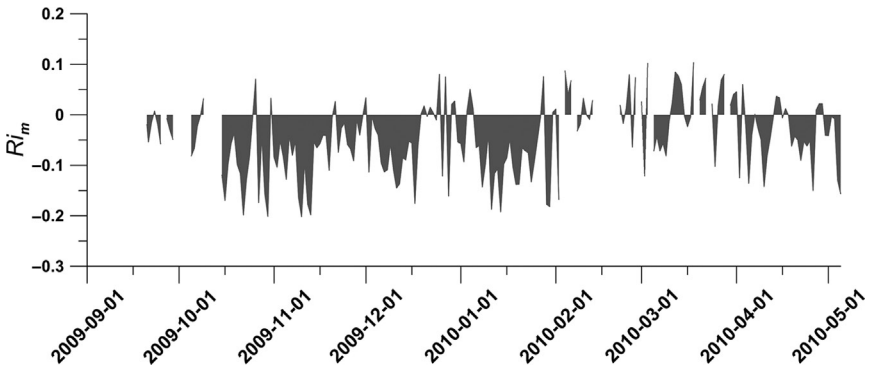

Fig. 6. Average daily atmospheric stability as the Richardson number, Ri_m, calculated from the CCT data. Positive numbers indicates stable boundary layer conditions and negative numbers indicate unstable conditions.

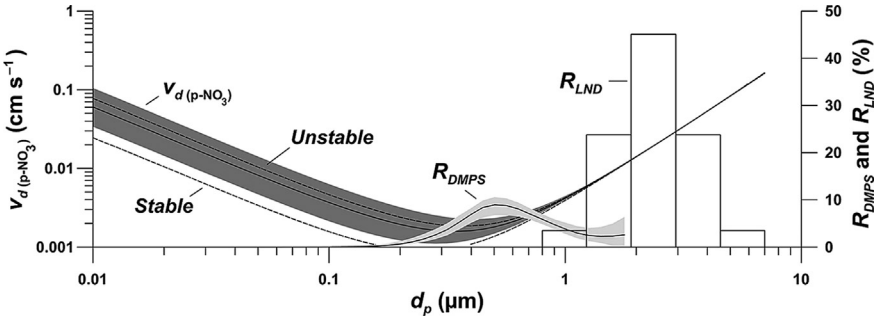

Fig. 7. Particulate median dry deposition velocities, $v_{d\ (p-NO_3)}$, for all particle diameters, d_p, estimated by the model and the corresponding median when only stable ($R_i > 0$) or unstable ($R_i < 0$) atmospheric conditions have been included (lower and upper dashed lines). The aerosol volume fraction, R_{DMPS}, measured by the Differential Mobility Particle Sizer (DMPS) at the Zeppelin atmospheric monitoring station, and the ratio, R_{LND}, between the five lognormal distributed (LND) size bins used to evaluate dry deposition of supermicron particles are also given. Shaded areas indicate 1st and 3rd quartiles of modelled output and measured R_{DMPS}.

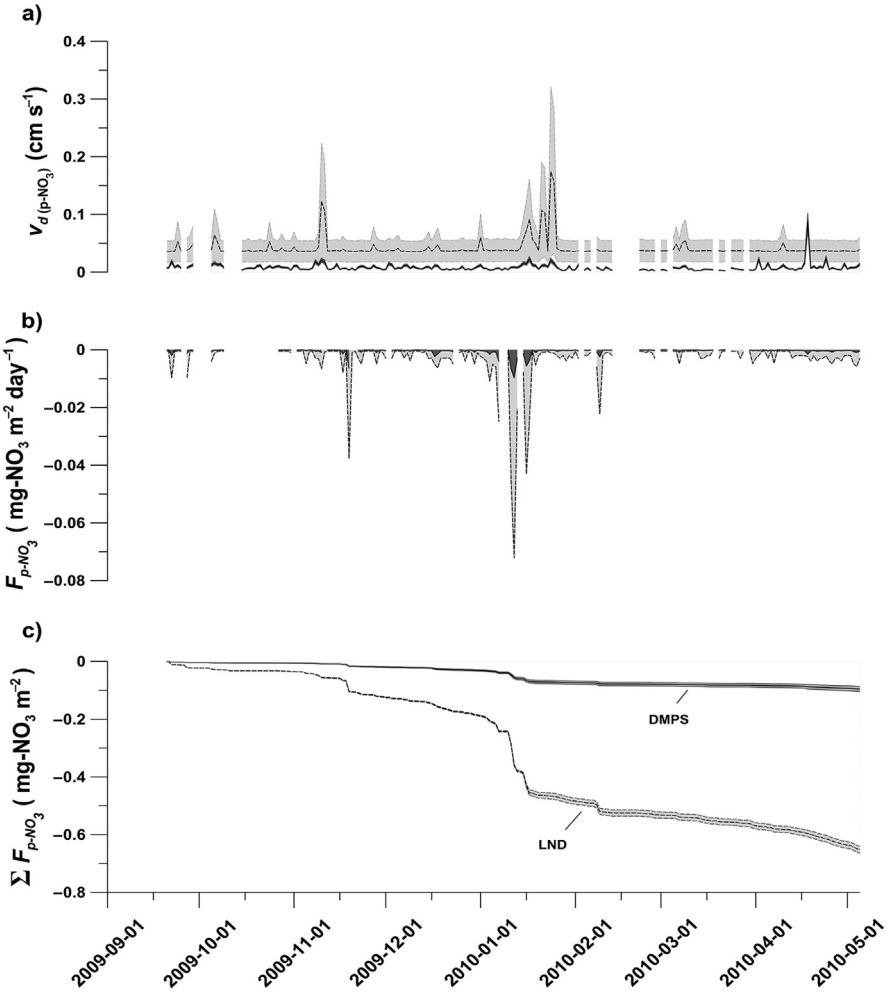

Fig. 8. Dry deposition of p-NO_3 during Winter 2009–2010 for the two model runs, using the range estimated from the Differential Mobility Particle Sizer (DMPS) or the lognormal distributed (LND) range among supermicron particles: a) daily average deposition velocity ($v_{d\ (p-NO_3)}$) for the two model runs, b) daily average dry deposition of p-NO_3 (F_{p-NO_3}) calculated from the $C_{p\text{-}NO_3}$ (Fig. 4b) and $v_{d(p\text{-}NO_3)}$, and c) the accumulated dry deposition (ΣF_{p-NO_3}) giving the total deposition for the winter season. The shaded areas in a) and c) indicate standard error of the estimates, while the shaded area in b) resembles the integrated area for the estimated dry deposition.

The standard error and spread of data presented here is only estimated from the actual modelled numbers. Errors in wind and temperature measurements are not included, neither are any errors in the measured atmospheric concentrations. A common feature for HNO_3 and p-NO_3 concentrations measured in the Arctic is that they usually present very low values, frequently below the detection limit of the filter method. In this data set detection limits were between 0.02 and 0.03 μg-N m^{-3} for both HNO_3 and p-NO_3. As a general rule data below the detection limit has been replaced with a number corresponding to 50% of the given detection limit.

Interestingly, the modelled dry deposition flux shows a strong influence of the variability in measured atmospheric concentrations for both HNO_3 and p-NO_3. This indicates an episodic behaviour of dry deposition, a pattern that has recently been shown to be important for total nitrate deposition in precipitation (Kühnel et al., 2011), with suggested importance for glacial ecosystems (Hodson et al., 2005; Hodson et al., 2009; Roberts et al., 2010). Back trajectories were run for the 18 days with highest atmospheric concentrations (sum of HNO_3 and p-NO_3) to see the influence of direct transport upon these periods (not shown). Direct transport of pollutants from Europe and Russia has previously been suggested to be an important factor in the Svalbard atmospheric composition (Rahn et al., 1980; Dickerson, 1985; Stohl et al., 2007; Hirdman et al., 2010) and precipitation (Hodson et al., 2005; Krawczyk et al., 2008; Kühnel et al., 2011). However, only 8 out of these 18 days indicate back trajectories from the European and Russian regions suggesting other processes (e.g. ocean emission, local pollutant events or other source regions, or other Arctic processes) might be of importance as well. Trajectories were obtained from the FLEXTRA model provided by NILU[4].

3.4. Estimating total dry deposition on Austre Brøggerbreen

To estimate the importance of dry deposition on a catchment scale, the output from each method was scaled up and compared with total deposition on Austre Brøggerbreen. The total deposition was calculated from the slope of eq. (4), $y = 170.49(\pm 23.90)x + 30.68(\pm 12.00)$ in Fig. 3 and was scaled to the winter accumulation rate measured by the Norwegian Polar Institute (J. Kohler, personal communication). The total area of Austre Brøggerbreen is assumed to be 6.12 km^2 where the winter accumulation (Table 4), measured as SWE, ranges from 0.42 to 0.73 m depending on glacial elevation (Table 4). The total nitrate accumulation on the glacier was then calculated to be 780.54 ± 156.54 kg (Table 4). In line with earlier discussion both dry and wet deposition along with post depositional processes will contribute to this total accumulation. Using the estimates for dry deposition across the snow season and scaling this to the areal cover of Austre Brøggerbreen, a deposition of -62.85 ± 23.50, -187.76 ± 73.44 and -65.85 ± 7.71 kg NO_3 was calculated using snow tray, glacial accumulation and the corrected LND-model results, respectively (Table 5). This would correspond to $8.05 \pm 3.01\%$, $24.06 \pm 9.41\%$ and $8.44 \pm 0.99\%$ of the total nitrate deposition (Table 5).

Table 4. Winter snow accumulation on Austre Brøggerbreen for Winter 2009–2010 and the corresponding load of NO_3 calculated from the data given in Fig. 3

Elevation interval* (m.a.s.l.)	Area* (km^2)	SWE* (m)	NO_3 per SWE (mg m^{-2})	Total NO_3 (kg interval^{-1})
50–100	0.03	0.42	102.29 ± 22.04	3.07 ± 0.66
100–150	0.31	0.45	107.40 ± 22.76	33.29 ± 7.05
150–200	0.71	0.48	112.52 ± 23.47	79.89 ± 16.67
200–250	0.95	0.51	117.63 ± 24.19	111.75 ± 22.98
250–300	0.92	0.54	122.74 ± 24.91	112.93 ± 22.91
300–350	1.02	0.58	129.56 ± 25.86	132.16 ± 26.38
350–400	0.79	0.61	134.68 ± 26.58	106.40 ± 21.00
400–450	0.56	0.64	139.79 ± 27.30	78.28 ± 15.29
450–500	0.46	0.67	144.91 ± 28.01	66.66 ± 12.89
500–550	0.25	0.70	150.02 ± 28.73	37.51 ± 7.18
550–600	0.12	0.73	155.14 ± 29.45	18.62 ± 3.53
Total	6.12	–	–	780.54 ± 156.54

*Jack Kohler, unpublished data.

The snow tray and model methods attribute 8–9% of the total nitrate deposition to dry deposition and are in agreement within one standard error. These results are in the lower range of a recent model investigation of eight rural sites in Canada where the individual ratio of wet and dry deposition ranged between 8 and 55% (Zhang et al., 2009). Even though the snow tray and the model methods are in agreement, the comparison raises some questions. As seen in eq. (5) the dry deposition is influenced by both the deposition velocity and the atmospheric concentrations. During the field campaign there were no very high concentration events (Fig. 4), which might indicate that the extrapolation of the snow tray method underestimates the seasonal dry deposition for the winter 2009–2010 and instead represents the background dry deposition to the Ny-Ålesund region.

The glacial accumulation method predicts a higher dry deposition, compared with the snow tray and model methods, contributing with approximately 24% of the total deposition. This number is in the lower part of the 20 to 40% range earlier estimated for some sites on Greenland

[4]Available online: *http://tarantula.nilu.no/trajectories/index.cfm*

Table 5. Total dry deposition of NO_3^- at Austre Brøggerbreen calculated from the three different methods, with ± 1 SE indicated. The corresponding percentage of total deposition based on the measured 780.54 ± 156.54 kg (Table 4) deposition on Austre Brøggerbreen is also given

	Snow Tray	Glacial Accumulation	Model		
	F_{tray}	F_d	F_{HNO_3}	F_{p-NO_3} (LND)	Model sum
Total dry deposition (kg)	-62.85 ± 23.50	-187.76 ± 73.44	-50.00 ± 6.23	-3.98 ± 0.06	-53.98 ± 6.30
			-61.02 ± 7.65#	-4.83 ± 0.06#	-65.85 ± 7.71
% of total deposition	8.05 ± 3.01	24.06 ± 9.41	6.41 ± 0.80	0.51 ± 0.01	6.92 ± 0.81
			7.82 ± 0.98#	0.62 ± 0.01#	8.44 ± 0.99

#Data corrected for the 22% paucity.

(Fischer and Wagenbach, 1996), where low snow accumulation rates might explain the relatively high contribution of dry deposition (Cadle, 1991).

The results of all three methods are in agreement if an uncertainty margin of ± 2 S.E.'s (approximately equal to a 95% confidence interval) is considered and results in an average dry deposition of 13.5% of the total deposition with an estimated range from 2.0 to 43.9% using this ± 2 SE assumption.

4. Conclusions

Nitrate dry deposition was estimated to account for $\sim 14\%$ of the total nitrate deposition at the glacier Austre Brøggerbreen, Svalbard, using three different methods with an overall agreement using a ± 2 standard errors. The total result range of the methods runs from 2 to 44% where the glacial accumulation method predicts relatively higher values and a larger spread with respect to modelled results and snow tray measurements.

The average atmospheric loss and subsequent nitrate contribution to the surface was estimated to be -10.27 ± 3.84, -30.68 ± 12.00 and -10.76 ± 1.26 mg m^{-2} ($\pm$ S.E.) for the snow tray, glacial accumulation and model approach, respectively. Furthermore, the modelled dry deposition of HNO_3 (-9.97 ± 1.25 mg m^{-2}) exceeds that of p-NO_3 (-0.79 ± 0.01 mg m^{-2}) by one order of magnitude. Two separate calculations, using measured aerosol size distributions and assumed lognormal distributed sizes, demonstrate that the general particulate nitrate dry deposition only contributes up to 1–7% of the total nitrate dry deposition.

Interestingly, the model results of this study indicate that dry deposition is strongly influenced by episodic events, something that has recently also been highlighted for N_r deposition via precipitation in Ny-Ålesund (Kühnel et al., 2011). Further follow-up investigations involving continuous year-round dry deposition measurements would be necessary to truly understand the role these episodic events play over larger time scales.

Even though the proportion of dry deposition compared to total nitrate deposition in this high Arctic region is small, and lower than some other remote areas, it still provides an important input of nutrients to this nitrogen limited region.

The newly established CCT and the well-equipped facilities at the Zeppelin Station provide a unique possibility to model dry deposition of a variety of substances in the Arctic. However, a future emphasis on measuring aerosols in the supermicron sizes would improve the overall monitoring program.

The focus of this study has been on nitrate dry deposition. To receive a full view of the atmospheric nutrient load to Svalbard ecosystems, other nitrogen containing species would also need attention. Furthermore, emphasis on establishing an effective wet and dry deposition sampler suitable for Arctic conditions would greatly enhance the understandings of the fate of atmospheric pollutants in the Arctic.

5. Acknowledgements

As a part of the international project 'Sources, sinks and impacts of atmospheric nitrogen deposition in the Arctic' (NSINK), this project received financial support from an EU Marie Curie Initial Stage Training Network Award NSINK (FP7 215503) and fieldwork were supported by an Arctic Field Grant, Svalbard Science Forum. NILU's atmospheric monitoring program at the Zeppelin Station is financed by the Norwegian Climate and Pollution Agency and ITM's research at the same station is supported by the Swedish Environmental Protection Agency. This is also a contribution to 'Crysophere-Atmosphere interaction in a changing Arctic climate (CRAICC)' a Top-Level Research Initiative (TRI). Logistic support was provided by the Norwegian Polar Institute staff at the Sverdrup Station, Ny-Ålesund, while A. Nowak-Zwierz, K. A. Kozio and C. L. Chakrabarti contributed to the analytical work in Sheffield, and J. Kohler kindly provided snow accumulation data from Austre Brøggerbreen.

References

Aas, W., Manø, S., Solberg, S. and Yttri, K. E. 2011. Monitoring of long-range transported air pollutants. Annual Report for 2010 [In Norwegian]. *OR 29/2011(Klif report 1099/2011)*. Norwegian Institute for Air Research, Kjeller, Norway.

Abbatt, J. P. D. 1997. Interaction of HNO_3 with water-ice surfaces at temperatures of the free troposphere. *Geophys. Res. Lett.* **24**, 1479–1482.

Albert, M. R. and Hardy, J. P. 1995. Ventilation experiments in a seasonal snow cover. *Biogeochemistry of Seasonally Snow-Covered Catchments, IAHS pub. no.* **228**, 44–49.

Albert, M. R., Grannas, A. M., Bottenheim, J., Shepson, P. B. and Perron, F. E. 2002. Processes and properties of snow-air transfer in the high Arctic with application to interstitial ozone at Alert, Canada. *Atmos. Environ.* **36**, 2779–2787.

Allen, M. D. and Raabe, O. G. 1982. Re-evaluation of millikan oil drop data for the motion of small particles in air. *J. Aerosol Sci.* **13**, 537–547.

Arya, S. P. 2001. *Introduction to Micrometeorology*. 2nd Edition. Academic Press, San Diego.

Bales, R. C., Davis, R. E. and Stanley, D. A. 1989. Ion elution through shallow homogeneous snow. *Water Resour. Res.* **25**, 1869–1877.

Barrie, L. A. 1986. Arctic air pollution: an overview of current knowledge. *Atmos. Environ.* **20**, 643–663.

Barrie, L. A. 1991. Snow formation and the processes in the atmosphere that influence its chemical composition. In: *Seasonal Snowpacks* (eds. T. D. Davies, M. Tranter and H. G. Jones). NATO ASI Series. Springer-Verlag, Berlin, pp. 1–20.

Barry, R. G. 1992. Climate-ice interactions. In: *Encyclopedia of Earth System Science* (ed. W.A. Nierenberg). Academic Press, San Diego, pp. 517–524.

Becagli, S., Proposito, M., Benassai, S., Gragnani, R., Magand, O. and co-authors 2005. Spatial distribution of biogenic sulphur compounds (MSA, $nssSO_4^{2-}$) in the northern Victoria land-dome c-wilkes land area, east Antarctica. *Ann. Glaciol.* **41**, 23–31.

Beine, H. J., Domine, F., Ianniello, A., Nardino, M., Allegrini, I. and co-authors 2003. Fluxes of nitrates between snow surfaces and the atmosphere in the European high Arctic. *Atmos. Chem. Phys.* **3**, 335–346.

Bergin, M. H., Jaffrezo, J. L., Davidson, C. I., Dibb, J. E., Pandis, S. N. and co-authors 1995. The contributions of snow, fog, and dry deposition to the summer flux of anions and cations at Summit, Greenland. *J. Geophys. Res.-Atmos.* **100**, 16275–16288.

Blunier, T., Floch, G. L., Jacobi, H. W. and Quansah, E. 2005. Isotopic view on nitrate loss in Antarctic surface snow. *Geophys. Res. Lett.* **32**. DOI: 10.1029/2005gl023011.

Brimblecombe, P., Tranter, M., Tsiouris, S., Davis, T. D. and Vincent, C. E. 1986. The chemical evolution of snow and meltwater. Modelling snowmelt-induced processes. In: *Proceedings of the Budapest Symposium, July 1986, IAHS Publ. no.* **155**, 283–295.

Cadle, S. H., Dasch, J. M. and Mulawa, P. A. 1985. Atmospheric concentrations and the deposition velocity to snow of nitric-acid, sulfur-dioxide and various particulate species. *Atmos. Environ.* **19**, 1819–1827.

Cadle, S. H. 1991. Dry deposition to snowpacks. In: *Seasonal Snowpacks* (eds. T. D. Davies, M. Tranter and H. G. Jones). Springer-Verlag, Berlin, pp. 21–66.

Colbeck, S. C. 1997. Model of wind pumping for layered snow. *J. Glaciol.* **43**, 60–65.

Cress, R. G., Williams, M. W. and Sievering, H. 1995. Dry depositional loading of nitrogen to an alpine snowpack, Niwot Ridge, Colorado. In: *Biogeochemistry of Seasonally Snow-Covered Catchments. IAHS Publ. no.* **228**, 33–40.

Dibb, J. E., Talbot, R. W., Munger, J. W., Jacob, D. J. and Fan, S. M. 1998. Air-snow exchange of HNO_3 and NO_y at Summit, Greenland. *J. Geophys. Res.-Atmos.* **103**, 3475–3486.

Dickerson, R. R. 1985. Reactive nitrogen-compounds in the Arctic. *J. Geophys. Res.-Atmos.* **90**, 10739–10743.

Diehl, K., Mitra, S. K. and Pruppacher, H. R. 1995. A laboratory study of the uptake of HNO_3 and HCL vapor by snow crystals and ice spheres at temperatures netween 0 and -40°C. *Atmos. Environ.* **9**, 975–981. DOI: 10.1016/1352-2310(95)00022-q.

Dore, A. J., Choularton, T. W. and Fowler, D. 1992a. An improved wet deposition map of the United-Kingdom Incorporating the seeder feeder effect over mountainous terrain. *Atmos. Environ. Part A* **26**, 1375–1381.

Dore, A. J., Choularton, T. W., Fowler, D. and Crossley, A. 1992b. Orographic enhancement of snowfall. *Environ. Pollut.* **75**, 175–179.

Durham, J. L. and Stockburger, L. 1986. Nitric acid – air diffusion coefficient: experimental determination. *Atmos. Environ.* **20**, 559–563. DOI: 10.1016/0004-6981(86)90098-3.

EMEP, 2001. EMEP Manual for sampling and chemical analysis. *EMEP/CCC-Report 1/1995 (last revision 2001)*. Norwegian Institute for Air Research, Kjeller, Norway. Online at: http://www.nilu.no/projects/ccc/manual/index.html

Fischer, H. and Wagenbach, D. 1996. Large-scale spatial trends in recent firn chemistry along an east-west transect through central Greenland. *Atmos. Environ.* **30**, 3227–3238.

Fischer, H., Wagenbach, P. and Kipfstuhl, J. 1998. Sulfate and nitrate firn concentrations on the Greenland ice sheet – 1. Large-scale geographical deposition changes. *J. Geophys. Res.-Atmos.* **103**, 21927–21934.

Forland, E. J. and Gjessing, Y. T. 1975. Snow contamination from washout-rainout and dry deposition. *Atmos. Environ.* **9**, 339–352.

Førland, E. J., Hanssen-Bauer, I. and Nordli, P. Ø. 1997. Climate statistics & longterm series of temperature and precipitation at Svalbard and Jan Mayen. **21/97**. The Norwegian Meteorological Institute.

Fowler, D., Cape, J. N., Leith, I. D., Choularton, T. W., Gay, M. J. and co-authors 1988. The influence of altitude on rainfall composition at Great Dun Fell. *Atmos. Environ.* **22**, 1355–1362.

Galloway, J. N., Aber, J. D., Erisman, J. W., Seitzinger, S. P., Howarth, R. W. and co-authors 2003. The nitrogen cascade. *Bioscience* **53**, 341–356.

Goto-Azuma, K., Nakawo, M., Jiankang, H., Watanabe, O. and Azuma, N. 1994. Melt-induced relocation of ions in glaciers and in a seasonal snowoack. In: *Proceedings of the Snow and Ice Covers: Interactions with the Atmosphere and Ecosystems*, Yokohama Symposia J2 and J5, 1994.

Goto-Azuma, K. and Koerner, R. M. 2001. Ice core studies of anthropogenic sulfate and nitrate trends in the Arctic. *J. Geophys. Res.-Atmos.* **106**, 4959–4969.

Granat, L. and Johansson, C. 1983. Dry deposition of SO_2 and NO_x in Winter. *Atmos. Environ.* **17**, 191–192.

Grannas, A. M., Jones, A. E., Dibb, J., Ammann, M., Anastasio, C. and co-authors 2007. An overview of snow photochemistry: evidence, mechanisms and impacts. *Atmos. Chem. Phys.* **7**, 4329–4373.

Gusev, A., Mantseva, E., Shatalov, V. and Travnikov, O. 2005. *Hemispheric model (MSCE-Hem) of persistent toxic substances dispersion in the environment*. MSC-E Tech. Note 11/2005. Co-operative programme for monitoring and evaluation of the long-range transmissions of air pollutants in Europe (EMAP). Moscow, Meteorological Synthesizing Centre East. Online at: http://www.msceast.org/reports/11_2005.pdf

Hara, K., Osada, K., Hayashi, M., Matsunaga, K., Shibata, T. and co-authors 1999. Fractionation of inorganic nitrates in winter Arctic troposphere: coarse aerosol particles containing inorganic nitrates. *J. Geophys. Res.-Atmos.* **104**, 23671–23679.

Harder, S. L., Warren, S. G., Charlson, R. J. and Covert, D. S. 1996. Filtering of air through snow as a mechanism for aerosol deposition to the Antarctic ice sheet. *J. Geophys. Res.-Atmos.* **101**, 18729–18743.

Hastings, M. G., Jarvis, J. C. and Steig, E. J. 2009. Anthropogenic impacts on nitrogen isotopes of ice-core nitrate. *Science* **324**, 1288. DOI: 10.1126/science.1170510.

Hicks, B. B., Baldocchi, D. D., Meyers, T. P., Hosker, R. P. and Matt, D. R. 1987. A preliminary multiple resistance routine for deriving dry deposition velocities from measured quantities. *Water, Air, Soil Pollut.* **36**, 311–330.

Hirdman, D., Sodemann, H., Eckhardt, S., Burkhart, J. F., Jefferson, A. and co-authors 2010. Source identification of short-lived air pollutants in the Arctic using statistical analysis of measurement data and particle dispersion model output. *Atmos. Chem. Phys.* **10**, 669–693.

Hodson, A. J., Mumford, P. N., Kohler, J. and Wynn, P. M. 2005. The high Arctic glacial ecosystem: new insights from nutrient budgets. *Biogeochemistry* **72**, 233–256. DOI: 10.1007/s10533-004-0362-0.

Hodson, A. J., Roberts, T. J., Engvall, A.-C., Holmén, K. and Mumford, P. N. 2009. Glacier ecosystem response to episodic nitrogen enrichment in Svalbard, European High Arctic. *Biogeochemistry* **98**, 171–184. DOI: 10.1007/s10533-009-9384-y.

Honrath, R. E., Peterson, M. C., Guo, S., Dibb, J. E., Shepson, P. B. and co-authors 1999. Evidence of NO_x production within or upon ice particles in the Greenland snowpack. *Geophys. Res. Lett.* **26**, 695–698.

Honrath, R. E., Lu, Y., Peterson, M. C., Dibb, J. E., Arsenault, M. A. and co-authors 2002. Vertical fluxes of NO_x, HONO, and HNO_3 above the snowpack at Summit, Greenland. *Atmos. Environ.* **36**, 2629–2640.

Huebert, B. J. and Robert, C. H. 1985. The dry deposition of nitric-acid to grass. *J. Geophys. Res.-Atmos.* **90**, 2085–2090.

Ianniello, A., Beine, H. J., Sparapani, R., Di Bari, F., Allegrini, I. and co-authors 2002. Denuder measurements of gas and aerosol species above Arctic snow surfaces at Alert 2000. *Atmos. Environ.* **36**, 5299–5309.

Ibrahim, M., Barrie, L. A. and Fanaki, F. 1983. An experimental and theoretical investigation of the dry deposition of particles to snow, pine trees and artificial collectors. *Atmos. Environ.* **17**, 781–788. DOI: 10.1016/0004-6981(83)90427-4.

Isaksson, E., Hermanson, M., Sheila, H. C., Igarashi, M., Kamiyama, K. and co-authors 2003. Ice cores from Svalbard – useful archives of past climate and pollution history. *Phys. Chem. Earth* **28**, 1217–1228. DOI: 10.1016/j.pce.2003.08.053.

Iversen, T. and Joranger, E. 1985. Arctic air-pollution and large-scale atmospheric flows. *Atmos. Environ.* **19**, 2099–2108.

Jacobi, H. W. and Hilker, B. 2007. A mechanism for the photochemical transformation of nitrate in snow. *J. Photochem. Photobiol., A* **185**, 371–382. DOI: 10.1016/j.jphotochem.2006.06.039.

Johannessen, M., Dale, T., Gjessing, E. T., A., H. and Wright, R. F. 1975. Acid precipitation in Norway: the regional distribution of contaminants in snow and the chemical concentration processes during snowmelt. In: *Proceedings of the Isotopes and Impurities in Snow and Ice; XVI Assembly of the International Union of Geodesy and Geophysics*, Grenoble, Switzerland, 1975.

Johansson, C. and Granat, L. 1986. An experimental-study of the dry deposition of gaseous nitric-acid to snow. *Atmos. Environ.* **20**, 1165–1170.

Krawczyk, W. E., Bartoszewski, S. A. and Siwek, K. 2008. Rain water chemistry at Calypsobyen, Svalbard. *Pol. Polar Res.* **29**, 149–162.

Kuhn, M. 2001. The nutrient cycle through snow and ice, a review. *Aquat. Sci.* **63**, 150–167.

Kumar, R., Srivastava, S. S. and Maharaj Kumari, K. 2008. Modeling dry deposition of S and N compounds to vegetation. *Indian J. Radio Space Phys.* **37**, 272–278.

Kvlividz, V. I., Kiselev, V. F. and Ushakova, L. A. 1970. Existence of Quasi-Liquid Layer on Ice Surface [*in Russian*]. *Dokl. Akad. Nauk SSSR* **191**, 1088–1090.

Kühnel, R., Roberts, T. J., Björkman, M. P., Isaksson, E., Aas, W. and co-authors 2011. Twenty-year climatology of NO_3^- and NH_4^+ wet deposition at Ny-Ålesund, Svalbard. *Advances in Meteorology* **2011**, 10. DOI: 10.1155/2011/406508.

Lilbaek, G. and Pomeroy, J. W. 2008. Ion enrichment of snowmelt runoff water caused by basal ice formation. *Hydrological Processes* **22**, 2758–2766. DOI: 10.1002/Hyp.7028.

Massman, W. J. 1998. A review of the molecular diffusivities of H_2O, CO_2, CH_4, CO, O_3, SO_2, NH_3, N_2O, NO, and NO_2 in air, O_2 and N_2 near STP. *Atmos. Environ.* **32**, 1111–1127.

Nilsson, E. D. and Rannik, U. 2001. Turbulent aerosol fluxes over the Arctic Ocean, 1. Dry deposition over sea and pack ice. *J. Geophys. Res.-Atmos.* **106**, 32125–32137.

Nordin, A., Schmidt, I. K. and Shaver, G. R. 2004. Nitrogen uptake by arctic soil microbes and plants in relation to soil nitrogen supply. *Ecology* **85**, 955–962.

Osada, K., Shido, Y., Iida, H. and Kido, M. 2010. Deposition processes of ionic constituents to snow cover. *Atmos. Environ.* **44**, 347–353. DOI: 10.1016/j.atmosenv.2009.10.031.

Petroff, A. and Zhang, L. 2010. Development and validation of a size-resolved particle dry deposition scheme for application in

aerosol transport models. *Geoscientific Model Development* **3**, 753–769. DOI: 10.5194/gmd-3-753-2010.

Rahn, K. A., Joranger, E., Semb, A. and Conway, T. J. 1980. High winter concentrations of SO_2 in the Norwegian Arctic and Transport from Eurasia. *Nature* **287**, 824–826.

Rasmussen, L. A. and Kohler, J. 2007. Mass balance of three Svalbard glaciers reconstructed back to 1948. *Polar Res*. **26**, 168–174. DOI: 10.1111/j.1751-8369.2007.00023.x.

Rattray, G. and Sievering, H. 2001. Dry deposition of ammonia, nitric acid, ammonium, and nitrate to alpine tundra at Niwot Ridge, Colorado. *Atmos. Environ*. **35**, 1105–1109.

Rinnan, R., Michelsen, A., Baath, E. and Jonasson, S. 2007. Fifteen years of climate change manipulations alter soil microbial communities in a subarctic heath ecosystem. *Glob. Change Biol*. **13**, 28–39. DOI: 10.1111/j.1365-2486.2006.01263.x.

Roberts, T. J., Hodson, A., Evans, C. D. and Holmen, K. 2010. Modelling the impacts of a nitrogen pollution event on the biogeochemistry of an Arctic glacier. *Ann. Glaciol*. **51**, 163–170. DOI: 10.3189/172756411795931949.

Robinson, D. A., Dewey, K. F. and Heim, R. R. 1993. Global snow cover monitoring – an update. *Bull. Am. Meteorol. Soc*. **74**, 1689–1696.

Seinfeld, J. H. and Pandis, S. N. 2006. *Atmosperic chemistry and physics: From air pollution to climate change*. 2nd ed. Hoboken, New Jersey, John Wiley & Sons.

Semb, A., Braekkan, R. and Joranger, E. 1984. Major ions in spitsbergen snow samples. *Geophys. Res. Lett*. **11**, 445–448.

Sharp, M., Skidmore, M. and Nienow, P. 2002. Seasonal and spatial variations in the chemistry of a High Arctic supraglacial snow cover. *J. Glaciol*. **48**, 149–158.

Shaver, G. R. and Chapin, F. S. 1980. Response to fertilization by various plant-growth forms in an Alaskan Tundra – nutrient accumulation and growth. *Ecology* **61**, 662–675.

Slinn, S. A. and Slinn, W. G. N. 1980. Predictions for particle deposition on natural-waters. *Atmos. Environ*. **14**, 1013–1016.

Slinn, W. G. N. 1982. Predictions for particle deposition to vegetative canopies. *Atmos. Environ*. **16**, 1785–1794.

Stohl, A. 2006. Characteristics of atmospheric transport into the Arctic troposphere. *J. Geophys. Res., [Atmos.]* **111**. DOI: 10.1029/2005jd006888.

Stohl, A., Berg, T., Burkhart, J. F., Fjaeraa, A. M., Forster, C. and co-authors 2007. Arctic smoke – record high air pollution levels in the European Arctic due to agricultural fires in Eastern Europe in spring 2006. *Atmos. Chem. Phys*. **7**, 511–534.

Ström, J., Umegard, J., Torseth, K., Tunved, P., Hansson, H. C. and co-authors 2003. One year of particle size distribution and aerosol chemical composition measurements at the Zeppelin Station, Svalbard, March 2000–March 2001. *Phys. Chem. Earth* **28**, 1181–1190. DOI: 10.1016/j.pce.2003.08.058.

Sturm, M. and Johnson, J. B. 1991. Natural-convection in the sub-Arctic snow cover. *J. Geophys. Res. [Solid Earth Planets]* **96**, 11657–11671.

Teinilä, K., Hillamo, R., Kerminen, V. M. and Beine, H. J. 2003. Aerosol chemistry during the NICE dark and light campaigns. *Atmos. Environ*. **37**, 563–575.

Teinilä, K., Hillamo, R., Kerminen, V. M. and Beine, H. J. 2004. Chemistry and modal parameters of major ionic aerosol components during the NICE campaigns at two altitudes. *Atmos. Environ*. **38**, 1481–1490. DOI: 10.1016/j.atmosenv.2003.11.028.

Travnikov, O. and Ilyin, I. 2005. Regional Model MSCE-HM of Heavy Metal Transboundary Air Pollution in Europe. *EMEP/MSC-E Technical Report 6/2005*. Meteorological Synthesizing Centre- ast. Moscow.

Wesely, M. L. 1989. Parameterization of surface resistances to gaseous dry deposition in regional-scale numerical-models. *Atmos. Environ*. **23**, 1293–1304.

Wesely, M. L. and Hicks, B. B. 2000. A review of the current status of knowledge on dry deposition. *Atmos. Environ*. **34**, 2261–2282.

Zhang, L., Vet, R., O'Brien, J. M., Mihele, C., Liang, Z. and co-authors 2009. Dry deposition of individual nitrogen species at eight Canadian rural sites. *J. Geophys. Res., [Atmos.]* **114**. DOI: 10.1029/2008jd010640.

Zieger, P., Fierz-Schmidhauser, R., Gysel, M., Ström, J., Henne, S. and co-authors 2010. Effects of relative humidity on aerosol light scattering in the Arctic. *Atmos. Chem. Phys*. **10**, 3875–3890.